

Investigation of volume distribution for pore water and pore air in partially saturated sand subjected to drying and wetting through morphological image processing

Ryunosuke Kido¹, Y. Higo², and F. Takamura²

¹ Department of Civil and Earth Resources Engineering, Kyoto University, Kyotodaigaku-Katsura, Nishikyo-ku, Kyoto, Japan.
(Research Fellow of Japan Society for the Promotion of Science)

² Department of Urban Management, Kyoto University, Kyotodaigaku-Katsura, Nishikyo-ku, Kyoto, Japan.

ABSTRACT

In the present study, water-retention states of partially saturated sand at different suction levels during water-retention test have been visualized by using microfocus X-ray CT. Morphological image processing such as erosion and dilation has been performed in this order for the pore water phase extracted from trinarised images in order to divide them into clusters having individual continuity. The variation in cluster volume distributions of the pore water and the pore air due to drying and wetting has been investigated, and then identification of water-retention states at different degrees of saturation are discussed from microscopic point of view.

Keywords: partially saturated sand; pore water; pore air; microfocus X-ray CT; morphological image processing

1 INTRODUCTION

Water-retention behavior of partially saturated soil is described as the relationship between matric suction and degree of saturation, which is referred to as soil water characteristic curve (SWCC). It is well known that a main drying curve is located above a main wetting curve called as hysteresis and water-retention state changes as wetting and drying, which significantly affect the mechanical and hydraulic behaviors of partially saturated soil. Water-retention behavior and mechanism of hysteresis have been macroscopically interpreted by using schematic illustration. It is however still necessary to investigate the partially saturated soil from microscopic point of view for better understanding the water-retention behavior.

Higo et al. 2015 has revealed by using microfocus X-ray CT with trinarisation for water-retention test that the relation between local porosity and local degree of saturation at almost the same global degree of saturation on drying path and wetting path is identical; thus, hysteresis is not attributed to the distribution of pore water with respect to porosity. On the other hand, the form of existing and volume distribution for pore air as well as those for pore water are not sufficiently investigated.

In the present study, water-retention states of partially saturated sand during drying process and wetting process have been visualized by using microfocus X-ray CT. Trinarisation technique has been applied to CT images obtained at the different suction levels for segmentation of the soil particle phase, the pore water phase and the pore air phase, respectively. Morphological image processing has been performed

for the pore water phase and the pore air phase extracted from the trinarised images in order to divide them into clusters.

The variation in cluster volume distributions of the pore water and the pore air during drying and wetting processes has been investigated. Those at almost the same degree of saturation in both processes is compared, by which the cause of hysteresis is discussed. Identification of water-retention state, which have been suggested by Bear 1979, is also discussed from microscopic point of view.

2 MATERIAL AND METHODS

2.1 The sample and testing program

The sample used in this study is Toyoura sand. The physical properties include a particle density of 2.64 g/cm³, a D₅₀ of 185 μm, a uniformity coefficient of 1.6, a fine content of 0.1 %, a maximum void ratio of 0.975 and a minimum void ratio of 0.614.

The specimen was prepared by water pluviation method with a void ratio of 0.637, D_r of 93.40% and a porosity of 38.91%. The size of the specimen was 20.00 mm in diameter and 20.07 mm in height. Suction was applied by negative water column technique, i.e., water head difference between top of the specimen and the water surface of burette connecting to the bottom of the specimen. The specimen was initially almost water-saturated condition, and then a main drying curve was firstly obtained by increasing suction. Similarly, a main wetting curve was obtained by decreasing suction.

Microfocus X-ray CT facility used in the present study is KYOTO-GEOμXCT extended by installing Flat Panel Detector (e.g. Higo et al. 2015). The middle

portion of the specimen was partially scanned at equilibrium states between a given suction and degree of saturation during water-retention test. Scanning time was about two hours. Voxel size of the obtained CT image was $5.4 \times 5.4 \times 7.0 \mu\text{m}^3$. The scan area was 5.5 mm in diameter and 5.87 mm in height.

2.2 Morphological image processing

Median filter with 5^3 voxels was applied to the CT images obtained during water-retention test to remove noises. Then, trinarisation by region growing technique, which takes partial volume effect into account (Kido et al. 2017), is performed in order to separate the three phases: the soil particle phase; the pore water phase; and the pore air phase, respectively. Local porosity and degree of saturation can be quantified by counting the number of voxels for each phase; however, it is unclear how the pore water and pore air exist.

In the present study, morphological image processing such as erosion, dilation and clustering is performed in this order for the binary images of the pore water phase extracted from the trinarised images, by which they are divided into clusters and then volume distribution is measured. Note that a cluster means a group composed of some voxels for the identical phase.

A conceptual illustration of erosion and dilation is depicted in Fig.1. In the present study, 6 voxels sharing each face of a voxel are considered as structuring elements of both the methods. In the case of erosion, the voxel for the pore water phase centered at the structuring element is replaced with one for the other phase when structuring element contains at least one voxel for the other phase. Dilation is just opposite processing of erosion: the voxel for the other phase at the structuring element is replaced with one for the pore water phase. The separated pore water subsequent to erosion and dilation is labeled by giving an identical intensity number to all adjacent voxels which makes up a cluster, by which the pore water phase is identified as clusters having individual continuity.

Through the coupling algorithm of morphological image processing, the volume distribution of the pore water phase can be evaluated without artifacts due to partial volume effect. Note that erosion and dilation are not applied to the pore air phase because there are probably few voxels for the pore air phase due to partial volume effect. An example of trinarised image and clustering image is shown in Fig.2. Each color shown in Fig.2 means identical number for each cluster.

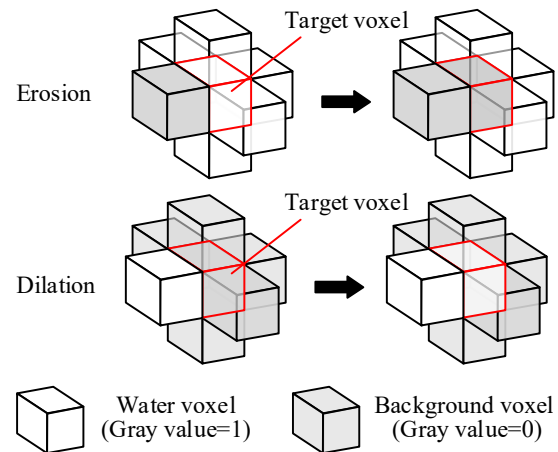


Fig.1 A conceptual illustration of erosion and dilation with structuring element of 6 voxels.

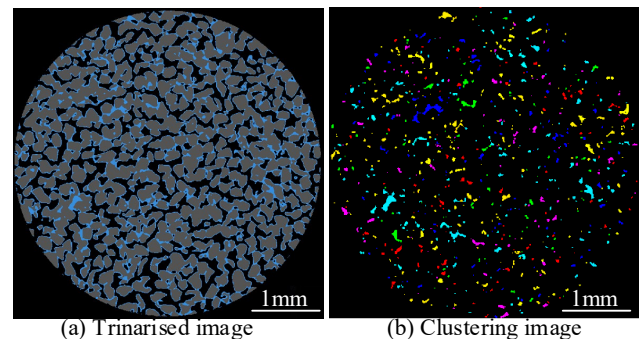


Fig.2 An example of trinarised image and clustering image.

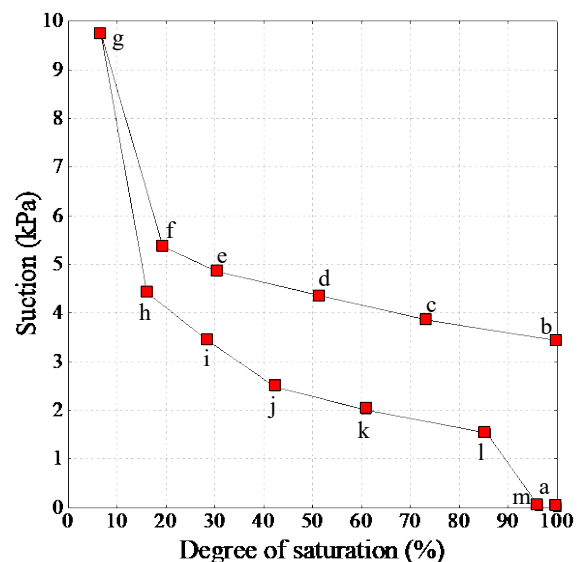


Fig.3 Soil water characteristic curve.

3 RESULTS AND DISCUSSIONS

SWCC obtained in the present study is shown in Fig.3. A drying curve is located above a wetting curve, i.e., hysteresis during drying and wetting processes is clearly observed. The alphabets in Fig.3 indicate the position where x-ray scan and image processing were

performed.

Fig.4 shows the horizontal slices of original CT images and the trinarised images at point “c” to “e” as drying process and “i” to “k” as wetting process. Gray, blue and black portions are the soil particle phase, the pore water phase and the pore air phase, respectively. Calculated local porosities are almost similar to global ones, whereas calculated local degrees of saturation are relatively larger than global ones, of which trend is consistent with Higo et al.2015. This is probably because of heterogeneous distribution of water content in the specimen: scanned portion contains relatively larger amount of water than the other portions.

Fig.5(a)(b) show the cluster volume distributions for the pore water and the pore air in drying process. Horizontal axis is the number of voxels which makes up each cluster as cluster volume, and vertical axis is frequency for each cluster, namely, the number of clusters with a given cluster volume. It is seen in Fig.5(a) that the lower degree of saturation is, the larger number of pore water clusters whose volume is smaller exists. It is also seen that a larger volume of pore water cluster than 10^7 voxels exists, and then it decreases with desaturation from “a” to “e”. Pore air shows a just opposite trend of pore water as shown in Fig.5(b). These indicate that a continuous pore water with larger volume mainly exists at higher degree of saturation, while the pore water loses its continuity as pore air volume increases and then pore air becomes continuous.

Fig.5(c)(d) show the cluster volume distributions for the pore water and the pore air in wetting process, which show the opposite trend of Fig.5(a)(b), i.e., pore water recovers continuity as saturation, and then pore air becomes discontinuous.

Fig.5(e)(f) show the comparisons of volume distributions for the pore water and the pore air at almost identical degrees of saturation on a main drying path and a main wetting path (“c” and “k”, “d” and “j”, “e” and “i”, “f” and “h”). It is found that volume distributions for both the phases in drying process are consistent with those in wetting process. It has been concluded in the previous research (Higo et al.2015) that pore water distribution with respect to local porosity at the similar degree of saturation in drying and wetting processes is identical even though water-retention curve shows hysteresis. It is therefore probable that hysteresis is attributed to geometry of pore water such as curvature rather than volume distributions for the pore air and the pore water.

It is however likely that water-retention states which have been explained by Bear 1979 are identified from microscopic point of view through image processing used in the present study. As shown in Fig.5, a continuous pore water and only smaller pore air exist at higher degree of saturation (“a”, “b”, “l”, “m”), which probably corresponds to insular-air saturation state. Both the pore water and the pore air can be continuous (“c”, “d”, “e”, “j”, “k”), which probably correspond to funicular saturation state. Finally, the form of existing only smaller pore water and a continuous pore air corresponds to pendular saturation state (“f”, “g”, “h”, “i”).

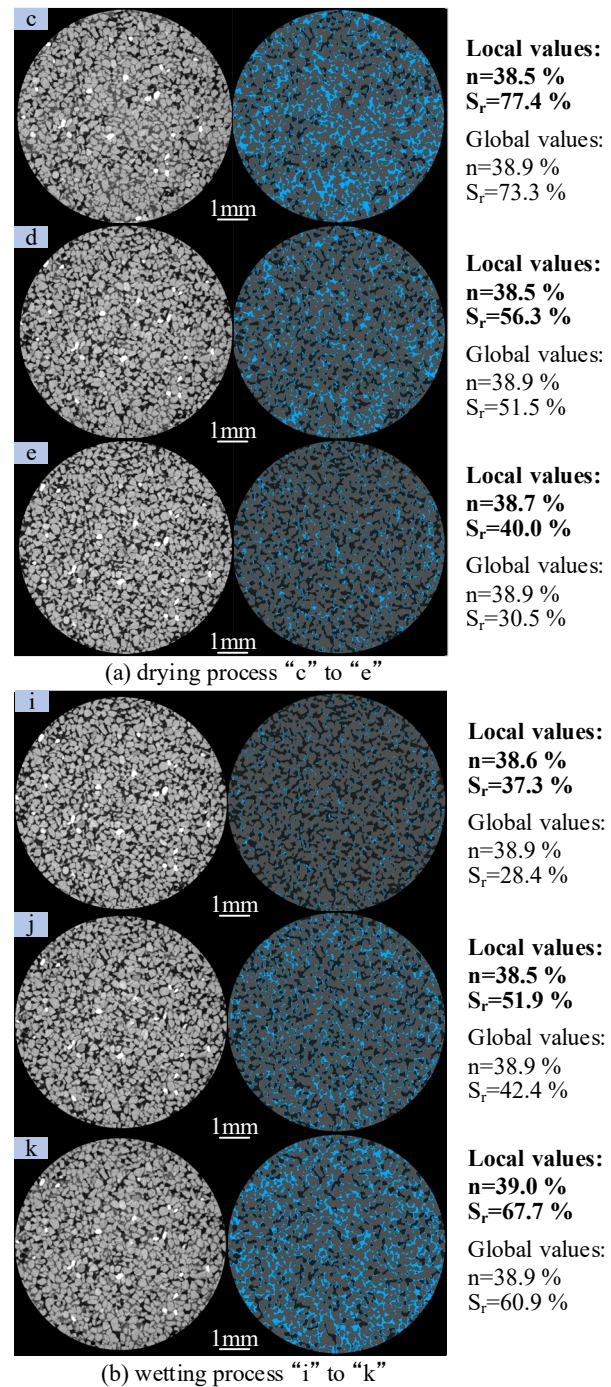


Fig.4 Horizontal slices of original CT images and trinarised images (a) drying process (b) wetting process.

4 CONCLUSIONS

Microfocus x-ray CT with morphological image processing for water-retention test have provided the volume distribution for the pore water phase and the pore air phase. It is found that the form of existing pore water and pore air changes as drying and wetting, and water-retention states can be identified through morphological image processing used in the present study. There is not significant difference in volume distribution for both the phases at almost the same

degree of saturation during drying and wetting processes. Further study on investigating geometry of pore water such as curvature is required to understand the mechanism of hysteresis.

REFERENCES

Bear, J. (1979). *Hydraulics of Groundwater*, New York, McGraw-Hill, 190-224.

Higo, Y., Morishita, R., Kido, R., Khaddour, G. and Salager, S. (2015). Local water-retention behavior of sand during drying and wetting process observed by micro x-ray tomography with trinarisation: The 15th Asian Regional Conference on Soil Mechanics and Geotechnical Engineering, Japanese Geotechnical Society Special Publication, 2(16), 635-638.

Kido, R. and Higo, Y. (2017). Evaluation of distribution of void ratio and degree of saturation in partially saturated triaxial sand specimen using micro x-ray tomography: International Mini Symposium CHUBU, Japanese Geotechnical Society Special Publication, 5(2), 22-27

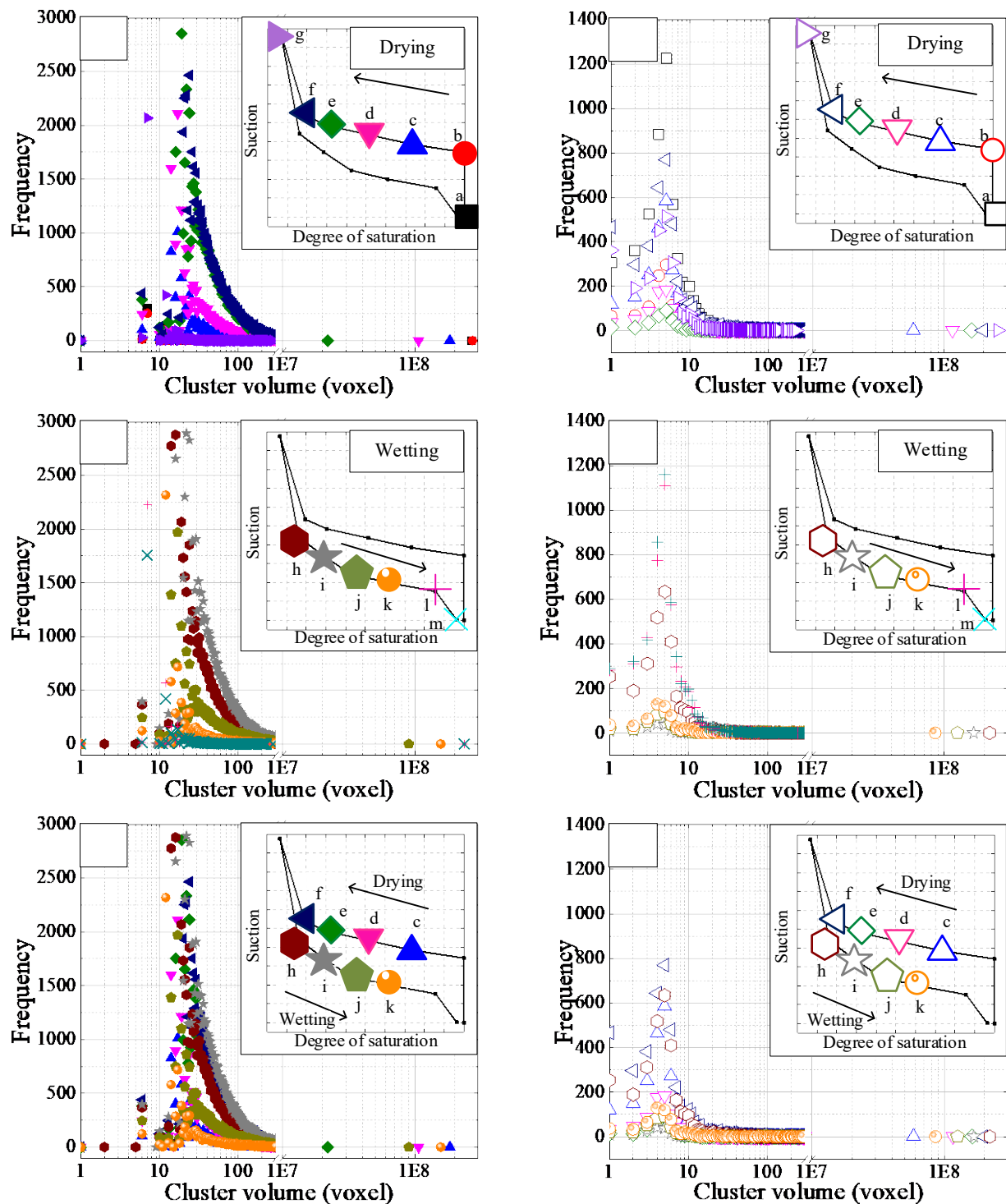


Fig.5 Cluster volume distributions of pore water ((a)(c)(e)) and pore air ((b)(d)(f)).